Study on Hydrolysis of Methyl Acetate in a Catalytic Distillation Column

WANG Chengxi(王成习)
Department of Chemical Engineering, Zhejiang University, Hangzhou 310027, China

Abstract A nonequilibrium stage model was used to simulate countercurrent multicomponent catalytic distillation processes for methyl acetate hydrolysis. Computations of stage efficiencies or height equivalent to a theoretical plate (HETP) were entirely avoided by this model. The consistency of simulated results and experimental data in conversions and concentration of each component along a column indicates that the model predicts the actual process well. The influences of operating parameters on hydrolytic conversions, such as feed molar ratios, feed locations, feed and reflux rates, heights of reactive and stripping sections, were analyzed adequately by simulating calculations. A good operating mode was then obtained, which is helpful to the development of a new process.
Keywords methyl acetate, hydrolysis, catalytic distillation, nonequilibrium stage model

1 INTRODUCTION

Processes combining chemical reaction and separation within one single apparatus are of increasing importance for industrial applications. Reactive distillation is one of these processes and especially offers a number of potential advantages[1]. Increasingly, it is performed in columns equipped with catalytic packings that combine the advantages of normal structured packing and heterogeneous catalysts. However, new types of structured catalytic packing were seldom reported. A plurality of closed cloth pockets containing a particulate catalytic material arranged and supported by wire mesh was used in methyl *t*-butyl ether (MTBE) production[2], but the utilization efficiency of catalyst is low.

Recently, a traditional operation of methyl acetate (MeAc) hydrolysis was investigated in order to discover possible improvement by catalytic distillation technology[3,4]. MeAc is a byproduct in industrial polyvinyl alcohol (PVA) plants. It is usually hydrolyzed to methyl alcohol (MeOH) and acetic acid (HAc) for recycle to polyvinyl acetate alcoholysis and vinyl acetate synthesis. The traditional recovery process (Fig. 1) comprises of a distillation column for separating alcoholyzed liquid mixture and a fixed-bed reactor packed with cation exchange resin followed by a complicated combination of several distillation columns for separation of each component. Because of the small value of equilibrium constant of hydrolytic reaction, conversion of MeAc is low (25%—31% for a traditional fixed-bed reactor) and a large portion of reactants must be recycled which results in a huge consumption of energy. A catalytic distillation column can be incorporated to replace the fixed-bed reactor, in which the equilibrium of hydrolytic reaction can be broken by the separation effect, so that a high hy-

drolytic conversion of MeAc will be obtained. This will be very favorable to decrease the following separation charge and energy consumption.
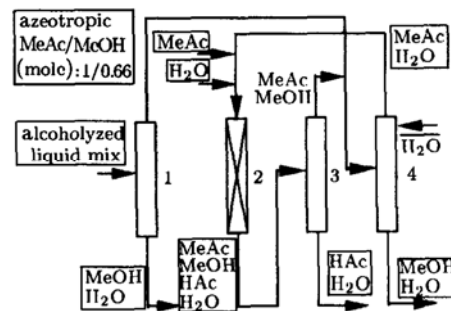

Figure 1 Traditional process of MeAc hydrolysis
1—distillation column; 2—hydrolysis reactor;
3—distillation column; 4—extractive distillation column

In this study, a new type of catalytic packing made from stainless steel rippled mesh and cation exchange membrane is used. Its characteristic in a catalytic distillation column is studied by a large number of experiments. Furthermore, a nonequilibrium stage model developed by Krishnamurthy and Taylor[5,6] is used to simulate the actual process of MeAc hydrolysis, in which reactive terms are added to the equations of component material and energy balances according to Zheng and Xu[7]. It is validated by experimental data. In addition, by choosing operating conditions arbitrarily in simulations, a more reasonable operating mode is proposed.

2 MATHEMATICAL MODEL AND EXPERIMENTAL VALIDATION

2.1 Experimental apparatus and mathematical model

A schematic diagram of the experimental appar

---

atus for MeAc hydrolysis is shown in Fig. 2. Its detailed structure is consistent with previous work[8]. There were two feed sites along the column. The overhead vapor was condensed completely and returned to the column, and the product was only discharged from the bottom still.
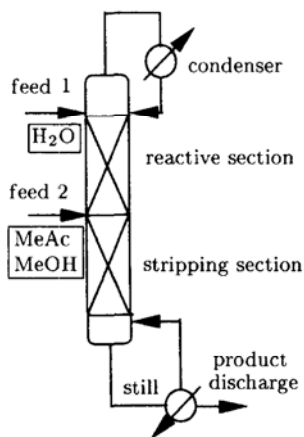

Figure 2   Catalytic distillation column
feed location: feed 1—1.8 m; feed 2—0.9, 1.2 or 1.8 m

The catalytic packing ($\phi 34\,\mathrm{mm} \times 50\,\mathrm{mm}$) installed in the reactive section (0.9 m long) was made from stainless steel rippled mesh and strong acidic cation exchange membrane with exchange capacity $2.0\,\mathrm{mmol \cdot g^{-1}}$. It is a cylindrical packing of sandwich. θ-ring inert packings ($\phi 3\,\mathrm{mm} \times 3\,\mathrm{mm}$) were filled in the stripping section (0.9 m long).

The bottom still is considered as an equilibrium stage. While the stripping and reactive sections are divided into sequence of nonequilibrium stages on account of short contact time between vapor and liquid in each stage. The nonequilibrium stage model is the same as that of Zheng and Xu[7] except the calculation method of mass transfer coefficients. In this model, phase equilibrium equations suggested by Sawistowski et al.[9] and Marek et al.[10,11] were used, the kinetic equation of hydrolysis was obtained in the previous work[12], the effective mass transfer coefficients were calculated based on the work of Krishnamurthy and Taylor[6], and binary mass transfer coefficients were calculated by Onda's correlations[13]. Other physical properties were evaluated using the methods suggested by Reid et al.[14] and Wang[12]. The calculation process is shown in Fig. 3.

2.2 Experimental validation

The experimental results under different operating conditions are summarized in Table 1, in which the hydrolytic conversions are calculated according to MeAc because it is the limited reactant (water is in excess). In addition, an azeotropic mixture feed (MeAc vs. MeOH molar ratio 1/0.66) was selected instead of pure MeAc in order to eliminate the extractive distillation column in Fig. 1.

As an adjustable parameter, the effective surface of the catalyst packing was calculated from the measured conversions. The ratios of a_e to a_p are shown in Table 1, and their average value is 0.472.
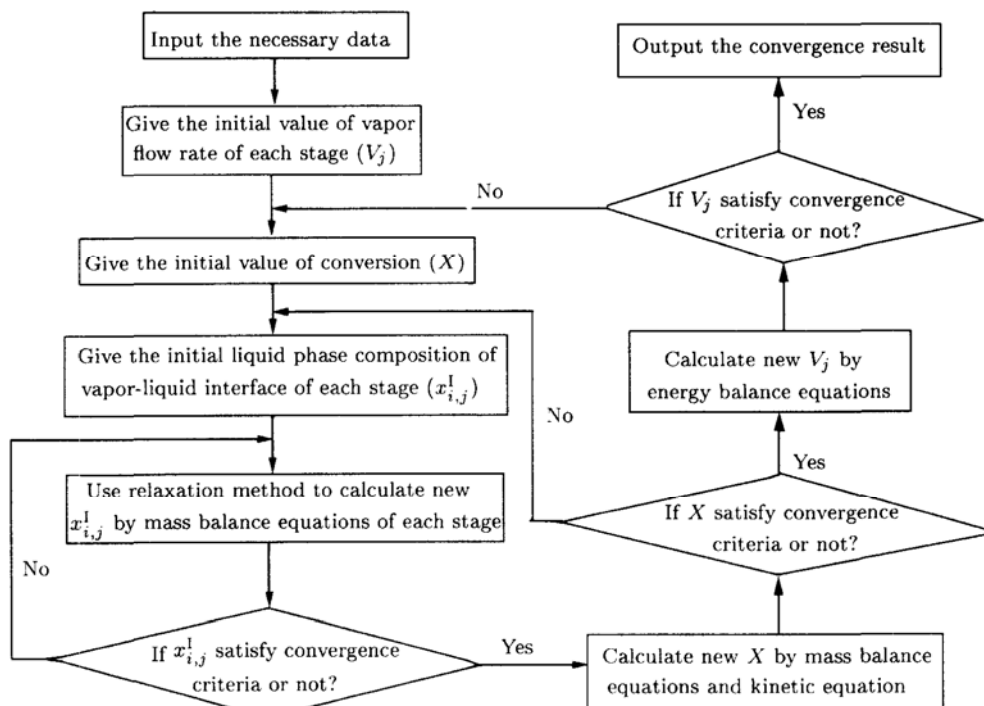

Figure 3   The calculation process of mathematical

Table 1   Experimental conditions and hydrolysis conversions (height of feed 1 : 1.8 m)

Run No.	Feed 1		Feed 2			Reflux		$H_2O/MeOH/MeAc$ (mole)	Conv., %		$\dfrac{a_e}{a_p}$
	Flow rate mol·h^{-1}	T °C	Flow rate mol·h^{-1}	T °C	Height m	Flow rate mol·h^{-1}	T °C		exp.	pred.	
1	1.898	25.0	1.589	20.0	0.9	6.271	30.0	1.19/0/1	31.24	31.88	0.430
2	3.143	30.0	0.973	15.0	0.9	8.615	30.0	3.23/0/1	69.73	71.09	0.444
3	4.615	30.0	1.044	15.0	0.9	7.812	30.0	4.42/0/1	80.40	81.27	0.457
4	6.041	30.0	1.079	15.0	0.9	9.007	30.0	5.60/0/1	92.15	91.05	0.488
5	3.748	8.0	1.216	8.0	0.9	10.58	8.0	3.39/0.1/1	68.72	68.85	0.470
6	3.694	11.0	1.155	11.0	0.9	11.80	11.0	3.52/0.1/1	72.04	71.12	0.486
7	2.660	40.0	1.310	25.0	0.9	13.11	30.0	3.11/0.532/1	64.98	64.60	0.479
8	2.526	8.0	1.219	8.0	0.9	11.80	8.0	3.17/0.530/1	68.95	66.98	0.505
9	2.526	8.0	1.024	8.0	0.9	11.80	8.0	3.77/0.528/1	80.12	79.48	0.482
10	1.558	15.0	1.328	20.0	0.9	8.348	30.0	1.93/0.648/1	47.03	47.17	0.471
11	3.967	30.0	1.377	15.0	0.9	8.744	35.0	4.81/0.669/1	84.48	89.13	0.416
12	5.630	30.0	1.390	15.0	0.9	7.675	35.0	6.75/0.666/1	98.40	99.57	0.430
13	5.321	20.0	2.102	15.0	0.9	7.675	25.0	4.07/0.608/1	64.30	65.31	0.457
14	5.468	30.0	2.185	15.0	0.9	12.36	25.0	4.08/0.630/1	70.01	66.75	0.523
15	8.701	35.0	2.357	20.0	0.9	7.538	30.0	5.97/0.617/1	72.92	69.44	0.527
16	8.269	35.0	2.280	18.0	0.9	12.90	30.0	5.77/0.591/1	78.56	77.50	0.486
17	2.538	20.0	2.110	20.0	0.9	5.875	30.0	2.07/0.720/1	40.98	42.58	0.417
18	2.932	15.0	1.378	10.0	0.9	8.093	25.0	3.63/0.704/1	75.04	74.89	0.478
19	2.039	12.0	1.772	12.0	1.8	6.271	12.0	2.04/0.772/1	36.93	36.33	0.491
20	1.818	20.0	1.320	20.0	1.8	7.812	20.0	2.27/0.645/1	45.72	46.15	0.461
21	4.507	20.0	1.851	20.0	1.8	6.984	25.0	3.88/0.593/1	59.57	58.44	0.493
22	3.151	20.0	1.149	20.0	1.8	8.744	20.0	4.45/0.621/1	81.00	81.50	0.467
23	4.975	30.0	1.279	30.0	1.8	7.402	25.0	6.38/0.639/1	97.15	95.31	0.498
24	2.328	20.0	1.490	14.5	1.2	9.392	25.0	2.57/0.645/1	53.45	53.25	0.476
25	3.062	25.0	1.211	14.5	1.2	9.392	25.0	4.16/0.645/1	77.84	81.37	0.428
26	4.784	25.0	1.564	14.0	1.2	8.093	25.0	5.01/0.638/1	83.60	81.64	0.499

Simulating each experiment again by using the average ratio of a_e to a_p, the comparison between experimental and predicted hydrolytic conversions is shown in Table 1. It is obvious that the predicted results are in good agreement with experimental ones.

The comparisons between experimental and predicted concentrations along the column for No. 20 and 26 are shown in Figs. 4 and 5 respectively, while those of products and reflux liquids are shown in Table 2. Evidently, the predicted results are also satisfactory.
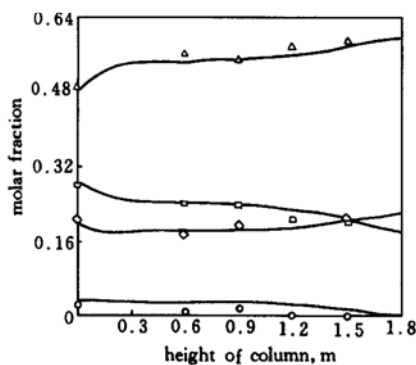
Figure 5   Comparison of experimental and predicted concentrations for No. 26
$\Diamond$ H_2O; $\triangle$ MeAc; $\square$ MeOH; $\bigcirc$ HAc; —prediction

Figure 4   Comparison of experimental and predicted concentrations for No. 20
$\Diamond$ H_2O; $\triangle$ MeAc; $\square$ MeOH; $\bigcirc$ HAc; —prediction

Table 2   Compositions of product and reflux

	Component	x, %			
		No. 20		No. 26	
		exp.	pred.	exp.	pred.
product	H_2O	47.48	46.36	63.38	62.85
	MeAc	12.64	14.00	2.17	2.51
	MeOH	28.35	28.07	21.42	22.11
	HAc	11.53	11.57	13.02	12.53
reflux	H_2O	8.69	9.34	11.45	13.91
	MeAc	73.43	71.84	79.57	76.92
	MeOH	17.88	18.82	8.98	9.19
	HAc	trace	trace	trace	trace

3 ANALYSIS OF PROCESS SIMULATION

In the following simulations, the temperatures of feed and reflux are 30℃.

3.1 Influence of water-to-MeAc molar ratio on hydrolytic reaction

From Fig. 6 we can find that the hydrolytic conversion of MeAc increases with the increase of water-to-MeAc molar ratio. Due to the high relative volatility of water-to-MeAc, the concentration of water is low in the liquid phase of the reactive section, which is very unfavorable to the hydrolytic reaction. In order to overcome this shortcoming, a more feasible method is to increase the feed rate of water at the top of the column.
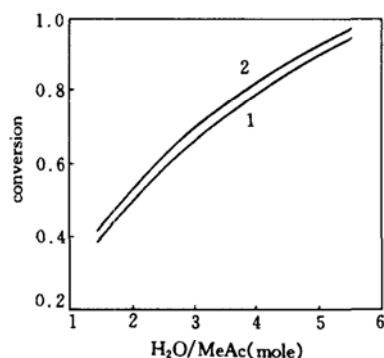
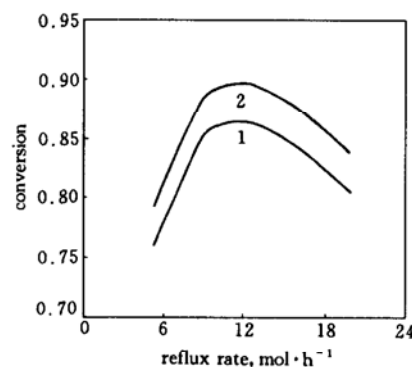**Figure 6 Effect of molar ratio of water-methyl acetate on conversion**
(feed location: feed 1—1.8 m; feed 2—0.9 m; MeAc feed rate: 0.9324 mol·h^{-1})
MeOH/MeAc(mole): 1—0.66/1; 2—0/1

Figure 7 Effect of reflux rate on conversion
(feed location: feed 1—1.8 mm; feed 2—0.9 m; MeAc feed rate: 0.9324 mol·h^{-1})
H$_2$O/MeOH/MeAc(mole): 1—4.5/0.66/1; 2—4.5/0/1

Figure 8 Effect of feed rate on conversion
[feed location: feed 1—1.8 m; feed 2—0.9 m; reflux rate: 9.0 mol·h^{-1}; H$_2$O/MeOH/MeAc(mole): 4.5/0.66/2]

3.2 Influence of reflux rate on hydrolytic reaction

Figure 7 shows that the hydrolytic conversion increases with the increase of the reflux rate at first, but as the reflux rate increases further, the conversion drops. It is obvious that there is a maximum in the range of simulated reflux rates. The concentrations of water and HAc in the liquid phase of the reactive section drop with the increase of reflux rate in a catalytic distillation operation. In this aspect it is quite different from traditional distillations for a total reflux operating system. The concentration drop of HAc is favorable to the hydrolytic reaction, while that of water is unfavorable to the reaction. Their cooperating action results in an optimal reflux rate.
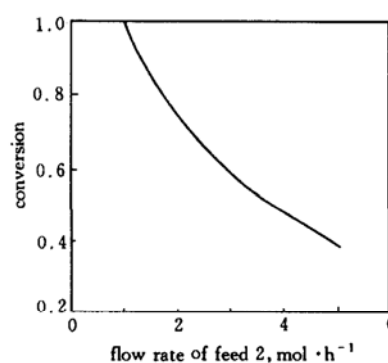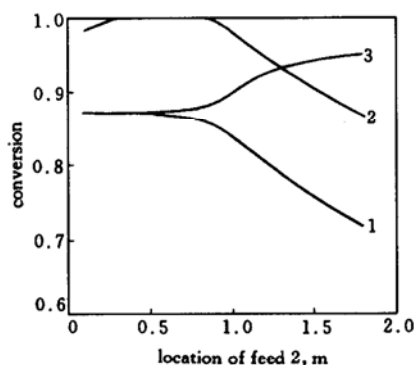
3.3 Influence of feed rate on hydrolytic reaction

Figure 8 shows that hydrolytic conversion decreases with the increase of feed rate in a wide range. A higher feed rate causes a shorter residence time, which is unfavorable to the hydrolytic process controlled by reaction.

3.4 Influence of feed location on hydrolytic reaction

As shown in Fig. 9, it is obvious that the optimal feed location of pure MeAc (curve 3) is at the top of the column, while that of MeAc and MeOH mixture is at the lower stripping section. For the hydrolysis system with higher conversion (curve 2), the optimal feed location for MeAc and MeOH azeotropic mixture is at the middle of the stripping section, otherwise, it will be at the bottom (curve 1).

From curves 1 and 3 in Fig. 9, we can find that if the feed location of MeAc and MeOH mixture is at the stripping section, there is hardly influence on hydrolytic conversion despite MeOH exist or not. The reason is that the feed location of the mixture is far from the reactive section, therefore, we can replace the pure feed of MeAc with MeAc and MeOH azeotrope in order to eliminate the extractive distillation column in Fig. 1. In other words, a catalytic distillation column can act as a reactor and an extractive distillation column simultaneously due to the feed of water from the top.

Figure 9   Effect of feed location of MeAc and MeOH
mixture on conversion
(location of feed 1: 1.8 m; reflux rate: $9.0 \, mol \cdot h^{-1}$)
MeAc feed rate, $mol \cdot h^{-1}$: 1,3—0.9324; 2—0.6289
$H_2O/MeOH/MeAc$(mole): 1,2—4.5/0.661/1; 3—4.5/0/1

3.5 Influence of packing depth on hydrolytic reaction

The simulated results for changing the packing depth of the reactive section, in which the amount of catalyst varies with depth, are shown in Fig. 10. We can find that hydrolytic conversion increases with the increase of catalytic packing depth. In addition, when the feed rate is lower, we can get nearly a 100% conversion by increasing the depth of catalytic packing. Otherwise, it is impossible to obtain higher conversion.
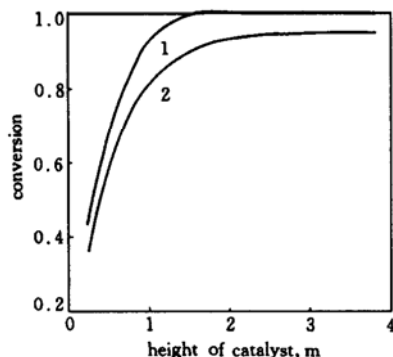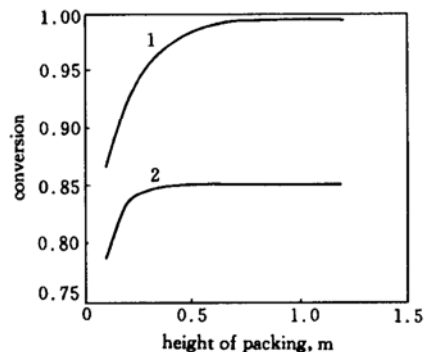

Figure 10   Effect of height of catalyst on conversion
[feed location: feed 1—top; feed 2—0.9 m;
reflux rate: $9.0 \, mol \cdot h^{-1}$; $H_2O/MeOH/MeAc$(mole):
4.5/0.66/1]
MeAc feed rate, $mol \cdot h^{-1}$: 1—15.5; 2—20.5

Figure 11 indicates that the packing depth of the stripping section has a large effect on conversions when the height of packing is lower. However, as the height of packing increases further, the hydrolytic conversion becomes constant.

Comparing the depths of reactive and stripping sections, we see that the required packing depth of the stripping section is much shorter in an actual catalytic distillation process.

Figure 11   Effect of height of stripping
section on conversion
[feed location: feed 1—top; feed 2—top of stripping section;
reflux rate: $9.0 \, mol \cdot h^{-1}$; $H_2O/MeOH/MeAc$ (mole):
4.5/0.66/1]
MeAc feed rate, $mol \cdot h^{-1}$: 1—10.4; 2—15.5

4 CONCLUSIONS

A nonequilibrium stage model is applied to simulate a catalytic distillation process of MeAc hydrolysis. The comparisons between the predicted and experimental results show that the model can approach the complex process well.

The predicted result shows that the hydrolytic conversion of MeAc increases as the total feed rate decreases, and also increases as the molar ratio of water-to-MeAc and the packing depths of reactive and stripping sections increase. There is an optimal reflux rate in the catalytic distillation process. The optimal feed location of MeAc is at the top of the reactive section in the absence of MeOH in the feed streams, and at the middle part or at the bottom of the stripping section in the presence of MeOH in the feed streams. The height of the stripping section may be lower than that of the reactive section. For the purpose of increasing the hydrolytic conversion of MeAc, the molar ratio of water-to-MeAc should not be too low. Besides, we can replace the pure feed of MeAc with MeAc and MeOH azeotrope in order to eliminate the extractive distillation column in the process.

NOMENCLATURE

a_e effective specific area of packing, m^{-1}
a_p specific area of packing, m^{-1}
V vapor flow rate, $mol \cdot h^{-1}$
x molar fraction of liquid phase
θ style of packing

Superscripts
I   interface of vapor-liquid phase

Subscripts
i component number
j stage number

REFERENCES

1 Degarmo, J. L., Parulekar, V. N., Pinjala, V., "Consider reactive distillation", *Chem. Eng. Prog.*, **88** (3), 43—50 (1992).

2 Simth, Jr., Tex, H., "Catalyst system for separating isobutene from C_4 streams", U.S. Pat., 4215011 (1979).

3 Fuchigami, Y., "Hydrolysis of methyl acetate in distillation column packed with reactive packing of ion exchange resin", *J. Chem. Eng. Japan.*, **23** (3), 354—359 (1990).

4 Kim, K. J., Roh, H. D., "Reactive distillation process and equipment for the production of acetic acid and methanol from methyl acetate hydrolysis", U.S. Pat., 5770770 (1998).

5 Krishnamurthy, R., Taylor, R., "A nonequilibrium stage model of multicomponent separation processes", *AIChE J.*, **31** (3), 449—465 (1985).

6 Krishnamurthy, R., Taylor, R., "Simulation of packed distillation and absorption columns", *Ind. Eng. Chem. Process Des. Dev.*, **24** (3), 513—524 (1985).

7 Zheng, Y. X., Xu, X. E., "Study on catalytic distillation processes", *Trans. Inst. Chem. Eng.*, **70** (A5), 459—470 (1992).

8 Wang, C. X., Qian, D. Y., Chen, W., Zhou, J. H., Chen, G. T., "Experimental study on methyl acetate hydrolysis by catalytic distillation", *Chemical Reaction Engineering and Technology*, **14** (2),179—184 (1998). (in Chinese)

9 Sawistowski, H., Pilavakis, P. A., "Vapor-liquid equilibrium with association in both phase multicomponent systems containing acetic acid", *J. Chem. Eng. Data.*, **27** (1), 64—71 (1982).

10 Marek, J., Standart, G., "Vapor-liquid equilibria in mixtures containing an associating substance I: Equilibrium relationships for systems with an associating component", *Collect. Czech. Chem. Commun.*, **19** (5), 1074—1081 (1954).

11 Marek, J., "Vapor-liquid equilibria in mixtures containing an associating substance II: Binary mixtures of acetic acid at atmospheric pressure", *Collect. Czech. Chem. Commun.*, **20** (6), 1490—1502 (1955).

12 Wang, C. X., "Study on applying catalytic distillation technique to the hydrolysis of methyl acetate", *Ph. D. Thesis*, Chem. Eng. Dept., Zhejiang University, Hangzhou (1997). (in Chinese)

13 Onda, K., Takeuchi, H., Okumoto, Y., "Mass transfer coefficients between gas and liquid phases in packed columns", *J. Chem. Eng. Japan*, **1** (1), 56—62 (1968).

14 Reid, R. C., Prausnitz, J. M., Poling, B. E., The Properties of Gases and Liquids, 4th edition. McGraw-Hill, New York (1987).